

Simplest cosmological model with the scalar field

A. Yu. Kamenshchik^{1†}, I. M. Khalatnikov^{1,2†} and A. V. Toporensky^{3*}

¹*L. D. Landau Institute for Theoretical Physics, Russian Academy of Sciences, Kosygin str. 2, Moscow, 117334, Russia*

²*Tel Aviv University, Tel Aviv University, Raymond and Sackler Faculty of Exact Sciences, School of Physics and Astronomy, Ramat Aviv, 69978, Israel*

³*Sternberg Astronomical Institute, Moscow University, Moscow, 119899, Russia*

We investigate the simplest cosmological model with the massive real scalar non-interacting inflaton field minimally coupled to gravity. The classification of trajectories in closed minisuperspace Friedmann-Robertson-Walker model is presented. The fractal nature of a set of infinitely bounced trajectories is discussed. The results of numerical calculations are compared with those obtained by perturbative analytical calculations around the exactly solvable minisuperspace cosmological model with massless scalar field.

PACS: 98.80.Hw, 98.80.Bp

† Electronic mail: kamen@landau.ac.ru

† Electronic mail: khalat@itp.ac.ru

* Electronic mail: lesha@sai.msu.su

I. Introduction

In recent years cosmological models with a scalar field acquired the great popularity because they can serve as a most natural basis for the inflationary cosmology¹. Indeed, the presence of scalar field in the model under consideration provides us with the existence of effective cosmological constant at the early stage of the cosmological evolution and with an opportunity to describe the decay of this constant and the “graceful exit” from inflation and transition to the Friedmann stage of evolution at a proper moment.

On the other hand scalar field is an integral part of modern models in particle physics. Moreover, the main part of papers devoted to quantum-cosmological description of the quantum origin of the Universe and to the definition and construction of the wave function of the Universe consider the models including scalar field which after the “birth” of the Universe is driving inflation²⁻⁴.

Side by side with the comparatively simple models based on the simple Lagrangians of the scalar field were developed rather complicated schemes considering the non-minimally coupled scalar field⁵, complex scalar field^{6,7} or the scalar field combining complexity and non-minimal coupling^{8,9}.

However, even the dynamics of the simple cosmological model, including gravity and minimally coupled scalar field with simple potential including only massive term is rather rich and deserves studying. The dynamics of the minisuperspace cosmological models with the massive real scalar field for the flat, open and closed Friedmann universes was studied in papers^{10,11} in terms of phase space and theory of dynamical systems. It was noticed that the dynamics of closed model (which is the most interesting from the quantum-cosmological point of view) is more complicated

than that dynamics of open and flat models. This dynamics allows the transitions from expansion to contraction and the existence of points of maximal expansion and minimal contraction in contrast with cases of open and flat cosmologies. Moreover, closed spherically symmetric models cannot expand infinitely and should have the points of maximal expansion provided the matter in the model under consideration satisfies the condition of energodominance ¹². The presence of points of maximal expansion and minimal contraction open the possibility for the existence of the trajectories of evolution of the Universe escaping singularity and oscillating in a periodical ¹³ or in an aperiodical ¹⁴ way between turning points. The possibility of existence of such trajectories or, in other words, non-singular universes filled with scalar field was discussed also earlier in Ref. 15.

Here we would like to consider the simplest cosmological model with massive real minimally coupled scalar field without self-interaction. We shall consider closed Friedmann model in minisuperspace including only two variables – cosmological radius a and homogeneous mode of inflaton scalar field φ . Because all the trajectories in such a model have the point of maximal expansion one can give the classification of the trajectories starting their evolution since these points. Studying such a classification we ignore the “prehistories” of the trajectories under consideration, i.e. we do not study their evolution before achieving points of maximal expansion. Such an approach simplifies the classification, because it gives us an opportunity to treat in the same way all the different kinds of trajectories – trajectories which exist during some finite intervals of time, i.e the trajectories which were born in singularity and disappear in it, the infinitely oscillating trajectories escaping falling into singularity and two kinds of “semi-infinite” trajectories which were either born in the singularity or disappear in it.

Suggested classification according to points of maximal expansion is convenient because localization of these points (i.e. a set of possible points of maximal expansion as well as those of minimal contraction) is well known and was described in Ref. 10 in terms of phase space and in Ref. 14 in terms of configuration space. General formulas describing such points for more wide class of models were presented in Ref. 9.

We shall distinguish trajectories which are monotonical in a and φ i.e. trajectories which fall to singularity with monotonically changing value of scalar field and the trajectories possessing bounces i.e points of minimal contraction when \dot{a} is equal to zero and trajectories having extrema in the value of scalar field φ – we shall call them φ -turns. It is remarkable that there is some regularity in the localization of the points of maximal expansion corresponding to different kinds of trajectories. The points is that the regions corresponding to trajectories falling to singularity after some definite number of φ -turns are separated by regions corresponding to bouncing trajectories. This phenomenon was detected by us due to numerical simulations and will be presented in detail in the second section.

Third section will be devoted to comparison of our model with even more simple model with massless scalar field ¹⁶. This model is of interest because it is exactly solvable and have only trajectories without bounces and φ -turns. So it is interesting to try to design some kind of perturbation theory for our model with massive scalar field where exactly solvable equations of motion for massless model play role of zero-order approximation. Such scheme seems promising because of interest to exactly solvable cosmological models rising in recent years ¹⁷. We shall see that for our model one can design such perturbative scheme and even to get the first-order corrections in an explicit way. However, this perturbation theory does not work in

the vicinity of singularity. Nevertheless, it will be shown that combining the solutions of equations of motion obtained in the framework of perturbation theory with some general properties of solutions of full (massive) theory one can obtain some useful information concerning different regimes of cosmological evolution. Perhaps, the approach developed in the present paper can be useful for analysis of the dynamical behavior of cosmological models which are close to some exactly solvable cases.

II. The model, equations of motion and their numerical investigation

We shall consider the cosmological model with an action

$$S = \int d^4x \sqrt{-g} \left\{ \frac{m_P^2}{16\pi} R + \frac{1}{2} g^{\mu\nu} \partial_\mu \varphi \partial_\nu \varphi - \frac{1}{2} m^2 \varphi^2 \right\}. \quad (2.1)$$

For the closed Friedmann model with the metric

$$ds^2 = N^2(t) dt^2 - a^2(t) d^2\Omega^{(3)}, \quad (2.2)$$

where $a(t)$ is a cosmological radius, N – a lapse function and $d^2\Omega^{(3)}$ is the metric of a unit 3-sphere and with homogeneous scalar field φ the action (2.1) takes the form

$$S = 2\pi^2 \int dt N a^3 \left\{ \frac{3m_P^2}{8\pi} \left[- \left(\frac{\dot{a}}{Na} \right)^2 + \frac{1}{a^2} \right] + \frac{\dot{\varphi}^2}{2N^2} - \frac{m^2 \varphi^2}{2} \right\}. \quad (2.3)$$

Now choosing the gauge $N = 1$ we can get the following equations of motion

$$\frac{m_P^2}{16\pi} \left(\ddot{a} + \frac{\dot{a}^2}{2a} + \frac{1}{2a} \right) + \frac{a\dot{\varphi}^2}{8} - \frac{m^2 \varphi^2 a}{8} = 0, \quad (2.4)$$

$$\ddot{\varphi} + \frac{3\dot{\varphi}\dot{a}}{a} + m^2 \varphi = 0. \quad (2.5)$$

Besides, we can write down the first integral of motion of our system

$$- \frac{3}{8\pi} m_P^2 (\dot{a}^2 + 1) + \frac{a^2}{2} (\dot{\varphi}^2 + m^2 \varphi^2) = 0. \quad (2.6)$$

It is easy to see from Eq. (2.6) that the points of maximal expansion and those of minimal contraction, i.e. the points, where $\dot{a} = 0$ can exist only in the region where

$$\varphi^2 \leq \frac{3}{4\pi} \frac{m_P^2}{m^2 a^2}, \quad (2.7)$$

which represents the field in the half-plane $0 \leq a < +\infty, -\infty < \varphi < +\infty$ restricted by hyperbolic curves $\varphi \leq \sqrt{\frac{3}{4\pi} \frac{m_P}{ma}}$ and $\varphi \geq -\sqrt{\frac{3}{4\pi} \frac{m_P}{ma}}$ (see Fig. 1). Sometimes, region defined by nonequalities (2.7) is called Euclidean or “classically forbidden”. One can argue about validity of such definition (see, for detail Ref. 9), but we shall use it for brevity. Now we would like to distinguish between points of minimal contraction where $\dot{a} = 0, \ddot{a} > 0$ and those of maximal expansion where $\dot{a} = 0, \ddot{a} < 0$. Let us put $\dot{a} = 0$, in this case one can express $\dot{\varphi}^2$ from Eq. (2.6) as

$$\dot{\varphi}^2 = \frac{3}{4\pi} \frac{m_P^2}{a^2} - m^2 \varphi^2. \quad (2.8)$$

Substituting (2.8) and $\dot{a} = 0$ into Eq. (2.4) we have

$$\ddot{a} = \frac{4\pi m^2 \varphi^2 a}{m_P^2} - \frac{2}{a}. \quad (2.9)$$

From Eq. (2.9) one can easily see that the possible points of maximal expansion are localized inside the region

$$\varphi^2 \leq \frac{1}{2\pi} \frac{m_P^2}{m^2 a^2} \quad (2.10)$$

while the possible points of minimal contraction lie outside this region (2.10) being at the same time inside the Euclidean region (2.7) (see Fig. 1).

We shall consider the trajectories beginning at some points of maximal expansion in the region defined by (2.10). As it has been already mentioned in the Introduction we shall trace out only the parts of the trajectories beginning since the points of maximal expansion ignoring their “prehistories”.

For the velocities $\dot{\varphi}$ defined by Eq. (2.8) we choose direction “up”, i.e. positive sign (the picture with velocities $\dot{\varphi}$ pointed out “down” can be obtained by mirror reflection in respect to axis $\varphi = 0$). Numerical investigation shows that for the points of maximal expansion placed in the region denoted in Fig. 2 by number **0** trajectories monotonically approach to singularity $a = 0, \varphi = +\infty$ (some typical trajectories of this kind are shown in Fig. 3a). It looks quite natural because in the region close to the ordinate axis $a = 0$ behavior of our system is close to that for the system with massless scalar field where bounces and φ -turns are absent. Then trajectories beginning in the region denoted in Fig. 2 by number **1** have a bounce. The typical trajectories of this kind are shown in Fig. 3b. Then we have region which we shall denote by number $\bar{1}$. In this region we also have a bounce, but before this bounce we have φ -turn. The typical trajectories beginning in the region $\bar{1}$ are shown on Fig. 3d. The boundary between the regions **1** and $\bar{1}$ is the place where some periodical trajectories escaping singularity can have their points of maximal expansion (such trajectories were first mentioned in Ref. 13 and analyzed in detail in Ref. 14). In particular, through the point $\varphi = 0$ lying on the boundary between the regions **1** and $\bar{1}$ goes the symmetric in φ periodic trajectory depicted in Fig. 3c.

In the region **1'** are localized the trajectories which have not a bounce, but φ -turn after that they tend to singularity $a = 0, \varphi = -\infty$ (see Fig. 3e). The boundary between the regions $\bar{1}$ and **1'** corresponds to trajectories where the points of bounce ($\dot{a} = 0, \ddot{a} > 0$) degenerates into inflection points ($\dot{a} = 0, \ddot{a} = 0$).

Then in the region **2** (see Fig. 2) we have the points of the maximal expansion for trajectories which after going through φ -turn have a bounce at $\varphi < 0$ escaping in such a way the fall into singularity (see Fig. 3f). In the region $\bar{2}$ we have the trajectories which have a bounce in the lower half-plane, just after two φ -turns. The

boundary between the regions **2** and $\bar{2}$ again contain trajectories including turning points where we have simultaneously $\dot{a} = 0, \dot{\varphi} = 0$. Some of these trajectories are periodical. One of such trajectories is shown in Fig. 3g.

Then starting since the point of maximal expansion in the region **2'** (see Fig. 2) we have the trajectories without bounces, but with two φ -turns (one at $\varphi > 0$ and one at $\varphi < 0$) after which they go to singularity $a = 0, \varphi = +\infty$ (see Fig. 3h).

Now one can easily understand what kind of trajectories corresponds to the points of maximal expansion localized in regions **3**, $\bar{3}$, **3'**, **4**, $\bar{4}$, **4'** and so on.

It is worth noticing that the most peculiar form has the boundary between the regions **1** and other regions in the upper half-plane ($\varphi > 0$). This boundary consists from two curves (see Fig.2). The left one is finite and divide the region **1** from the region $\bar{1}$ while the right curve is an infinite one and goes almost parallelly to the hyperbolic curve separating the possible points of maximal expansion from the possible points of minimal contraction (see Fig. 2). It is interesting that this upper curve touches all the regions beginning since $\bar{1}$.

In Fig. 3i is shown the trajectory whose point of maximal expansion is placed in the upper branch of the region **1**. This trajectory immediately after the bounce has φ - turn, then goes through the second point of maximal expansion falls into singularity in the lower half-plane.

All the regions beginning since $\bar{1}$ are compact in contrast with regions **0** and **1**.

Now one can pay attention to a special class of trajectories having the points of “full stop”, i.e. the points where $\dot{a} = 0, \dot{\varphi} = 0$ simultaneously. These points of full stop can lie only on the boundary between Euclidean and Lorentzian region. Naturally, the trajectories beginning with zero velocities at this boundary constitute the tiny minority in the set of all possible trajectories. Nevertheless it is interesting

to trace out the correspondence between the points of full stops of these trajectories and their points of maximal expansion. Here it is necessary to remember that in every point of maximal expansion we have two possible directions for $\dot{\varphi}$. Our classification was constructed for the direction “up”. The structure of regions corresponding to the direction “down” can be obtained by reflection of picture in respect to axis $\varphi = 0$. We shall distinguish between regions “up” and “down” by symbols \uparrow and \downarrow correspondingly.

Thus, let us consider the trajectories which begins with zero velocities $\dot{a} = 0, \dot{\varphi} = 0$ in the upper half-plane $\varphi > 0$. As was explained earlier the corresponding trajectories can have their points of maximal expansion on the curves separating the regions \mathbf{k} from the regions \bar{k} . Besides these boundaries the points of maximal expansion can be disposed on the infinite curve separating the region $\mathbf{1}$ from all other regions. Indeed, numerical investigation shows that the trajectories beginning at $0 < \varphi < \varphi_0$, go into Euclidean region and have the first point of maximal expansion just on this infinite curve separating the region $\mathbf{1}\uparrow$ from other regions Here φ_0 is the point where the direction of the motion at the initial moment coincides with the direction of the tangent to the curve given by an equality in (2.7) , i.e. the point where

$$\frac{\ddot{\varphi}}{\ddot{a}} = \frac{d\varphi}{da}. \quad (2.11)$$

Using Eqs. (2.4), (2.5),and (2.7) one can find

$$\varphi_0 = \sqrt{\frac{3}{4\pi}} m_P. \quad (2.12)$$

Then we consider trajectories beginning with zero velocities at $\varphi > \varphi_0$. Moving up the beginning of trajectory along the hyperbolic curve separating Euclidean and Lorentzian regions beginning since φ_0 we shall have the corresponding point of

maximal expansion moving down along the boundary between the regions $\mathbf{1}\uparrow$ and $\bar{\mathbf{1}}\uparrow$. Then, after approaching the final point of this curve (i.e. the crossing between this boundary curve and the curve separating the points of maximal expansion from points of minimal contraction) the closest to the beginning of motion point of maximal expansion jumps to some point of the boundary between regions $\mathbf{2}\downarrow$ and $\bar{\mathbf{2}}\downarrow$. Then while the beginning of the trajectory is moving up along the hyperbolic curve separating Euclidean and Lorentzian regions the corresponding point of maximal expansion is moving up to until the moment when it approaches to the curve separating the points of minimal contraction and maximal expansion in an upper half-plane. Then it jumps to some point on the curve separating the regions $\mathbf{3}\uparrow$ and $\bar{\mathbf{3}}\uparrow$ and so on and so forth. Thus we have seen that every point on the upper branch of the hyperbolic curve separating Euclidean and Lorentzian regions has a counterpart on one of curves separating regions \mathbf{k} and $\bar{\mathbf{k}}$ and the intervals denoted with sign “ \uparrow ” is interchanged with intervals denoted by that of “ \downarrow ”. The picture for the down part of hyperbolic curve disposed at $\varphi < 0$ will be quite the same with an only difference that signs \uparrow should be substituted by ones \downarrow and vice versa.

Now let us turn back to the analysis of the general set of trajectories in our problem. The most interesting for us will be trajectories which have bounces, and especially the trajectories which have a lot of bounces and as an ideal situation an infinite number of bounces (i.e. the trajectories escaping singularity).

Let us look at the trajectories whose points of maximal expansion are localized in the regions $\mathbf{1}, \mathbf{2}, \mathbf{3} \dots$, or in the regions $\bar{\mathbf{1}}, \bar{\mathbf{2}}, \bar{\mathbf{3}}, \dots$ i.e. the trajectories having at least one bounce. We shall study the structure of these regions from the point of view of localization of their second point of maximal expansion. The substructure of the region $\mathbf{1}\uparrow$ is represented on Fig. 4, while the forms of the trajectories corresponding

to various subregion of regions $\mathbf{1}$ and $\bar{\mathbf{1}}$ are presented in Fig. 5.

On the right near the boundary with the region $\bar{\mathbf{1}}$ we have subregion $\mathbf{1}\uparrow\bar{\mathbf{1}}\downarrow$ which corresponds to the trajectories which have after a bounce the second point of maximal expansion in the region $\bar{\mathbf{1}}\downarrow$ after which they have the second bounce. The next subregion to the left from the subregion $\mathbf{1}\uparrow\bar{\mathbf{1}}\downarrow$ is the subregion $\mathbf{1}\uparrow\mathbf{1}'\downarrow$ which corresponds to the trajectories which after bounce have the point of maximal expansion in the region $\mathbf{1}'\downarrow$. After this point of maximal expansion they have a φ -turn and then fall to singularity $a = 0, \varphi = -\infty$.

Then we have the subregion $\mathbf{1}\uparrow\mathbf{1}\downarrow$ which corresponds to trajectories with two bounces. Then we have subregion $\mathbf{1}\uparrow\mathbf{1}'\uparrow$. Then follows the subregions $\mathbf{1}\uparrow\mathbf{2}\uparrow, \mathbf{1}\uparrow\bar{\mathbf{2}}\uparrow, \mathbf{1}\uparrow\mathbf{2}'\uparrow, \mathbf{1}\uparrow\mathbf{1}\uparrow, \mathbf{1}\uparrow\mathbf{2}'\downarrow, \mathbf{1}\uparrow\mathbf{3}\downarrow$ and so on and so forth.

The structure of region $\bar{\mathbf{1}}\uparrow$ is much more simple: we have here only two subregions $\bar{\mathbf{1}}\uparrow\mathbf{1}\downarrow$ and $\bar{\mathbf{1}}\uparrow\mathbf{0}\downarrow$.

Thus inside the regions $\mathbf{1}\uparrow, \bar{\mathbf{1}}\uparrow$ we have an infinite set of subregions whose arrangement approximately repeat the structure of the whole field of the possible points of maximal expansion presented in Fig. 2.

One can see that the structure of couples of regions $\mathbf{2}\bar{\mathbf{2}}; \mathbf{3},\bar{\mathbf{3}}; \mathbf{4},\bar{\mathbf{4}} \dots$ is quite similar to that of couple of regions $\mathbf{1},\bar{\mathbf{1}}$.

Studying the structure of subregions corresponding to two bounces one can find inside each of them the same “substructure” of infinite set “subsubregions”. Continuing this procedure *ad infinitum* one can observe that the field of the localization of the points of maximal expansion corresponding to trajectories escaping singularity can be find as a result of an infinite procedure at each stage of each we encounter self-similar structures. Such a self-similarity of structures appearing at different scales points out on the fractal nature of the set obtained as the result of

infinite procedure ¹⁸. Thus, while the set of trajectories escaping singularity and infinitely oscillating between points of minimal contraction and maximal expansion has vanishing measure in the set of all possible trajectories it can at the same time have non-trivial fractal dimensionality. This phenomenon was first discussed in a little bit different terms in the paper by Page ¹⁴.

III. The cosmological model with the massless scalar field and the “anti-slow-roll” perturbation theory

We begin this paper with the rewriting of the equations (2.5) and (2.6) in terms of conformal time

$$\eta = \int dt \frac{1}{a(t)}$$

because in the conformal time the solutions for the corresponding equations of motion in massless limit can be written down explicitly. Thus, we have

$$\varphi'' + \frac{2\varphi'a'}{a} + m^2\varphi a^2 = 0 \tag{3.1}$$

and

$$\frac{a'^2}{a^2} = -1 + \frac{4\pi}{3m_P^2}\varphi'^2 + \frac{4\pi}{3m_P^2}m^2\varphi^2. \tag{3.2}$$

Here, “prime” denotes differentiation in respect to η . At $m = 0$ Eqs. (3.1) and (3.2) turn into

$$\varphi'' + \frac{2\varphi'a'}{a} = 0 \tag{3.3}$$

and

$$\frac{a'^2}{a^2} = -1 + \frac{4\pi}{3m_P^2}\varphi'^2. \tag{3.4}$$

These system of equations (3.3) and (3.4) can be exactly integrated. As in the preceding section we shall take as an initial moment of evolution that at which the

Universe is in the point of maximal expansion. Then we can get

$$a = a_0 \sqrt{\cos 2\eta}, \quad (3.5)$$

$$\frac{a'}{a} = -\tan 2\eta, \quad (3.6)$$

$$\varphi' = \sqrt{\frac{3m_P^2}{4\pi}} \frac{1}{\cos 2\eta}, \quad (3.7)$$

(here, we have chosen direction “up” for the evolution of scalar field just like in the preceding section) and, finally

$$\varphi = \varphi_0 + \frac{1}{4} \sqrt{\frac{3m_P^2}{4\pi}} \ln \frac{1 + \sin 2\eta}{1 - \sin 2\eta}. \quad (3.8)$$

These solutions correspond to trajectories which begin in one singularity $a = 0, \varphi = \pm\infty$ go through the point of maximal expansion $a = a_0, \varphi = \varphi_0$ and go to other singularity $a = 0, \varphi = \mp\infty$ (see Ref. 16). In terms of our Fig. 2 one can say that all half-plane (a, φ) is filled with the only region **0**.

Now, our purpose is to construct the perturbation theory for the solution of Eqs. (3.1) – (3.2) using the solution of massless equations (3.5)–(3.8) as zero-order approximation. Apparently, such perturbation theory is predestined for describing situations when the kinetic term in the Hamiltonian is much greater than the potential term in contrast with the well-known slow-roll approximation (see, for example, Ref. 7,19). Thus, we can call our scheme “anti-slow-roll approximation”. Again we choose as a starting moment for our evolution that moment, when the Universe is placed in the point of maximal expansion. For calculational simplicity we restrict ourselves by a symmetric case $\varphi(0) = 0$. It will be more convenient to consider instead of the variable a the variable h defined as

$$h \equiv \frac{a'}{a}. \quad (3.9)$$

When representing the solutions of equations of motion as

$$\varphi = \varphi^{(0)} + \delta\varphi \quad (3.10)$$

and

$$h = h^{(0)} + \delta h, \quad (3.11)$$

where $\varphi^{(0)}$ and $h^{(0)}$ are given by formulae (3.8) and (3.6) respectively, we can get the following equations for $\delta\varphi$ and δh :

$$\delta\varphi'' + 2\delta\varphi'h^{(0)} + 2\delta h\varphi^{(0)'} + m^2 a^{(0)2} \varphi^{(0)} \quad (3.12)$$

and

$$h^{(0)}\delta h = \frac{4\pi}{3m_P^2} \varphi^{(0)'} \delta\varphi' + \frac{4\pi}{3m_P^2} \frac{m^2 \varphi^{(0)2} a^{(0)2}}{2}. \quad (3.13)$$

Substituting into Eqs. (3.12), (3.13) explicit expressions for $\varphi^{(0)}$, $\varphi^{(0)'}$, $h^{(0)}$ and $a^{(0)}$ from Eqs. (3.5)–(3.8) we have

$$\delta\varphi'' - 2 \tan 2\eta \delta\varphi' + 2\delta h \sqrt{\frac{3m_P^2}{4\pi}} \frac{1}{\cos 2\eta} + \frac{1}{4} m^2 a_0^2 \cos 2\eta \sqrt{\frac{3m_P^2}{4\pi}} \ln \frac{1 + \sin 2\eta}{1 - \sin 2\eta} \quad (3.14)$$

and

$$h^{(0)}\delta h = \sqrt{\frac{4\pi}{3m_P^2}} \frac{1}{\cos 2\eta} \delta\varphi' + \frac{m^2 a_0^2}{32} \ln^2 \frac{1 + \sin 2\eta}{1 - \sin 2\eta}. \quad (3.15)$$

One can easily see from Eqs. (3.14) and (3.15) that the true small parameter in our perturbation theory is $m^2 a_0^2$.

Now one can using Eq. (3.15) express δh through $\delta\varphi$. We have

$$\delta h = -\sqrt{\frac{4\pi}{3m_P^2}} \frac{\delta\varphi'}{\sin 2\eta} - \frac{m^2 a_0^2 \cos^2 2\eta}{32 \sin 2\eta} \ln^2 \frac{1 + \sin 2\eta}{1 - \sin 2\eta}. \quad (3.16)$$

Substituting δh from Eq. (3.16) into Eq. (3.14) we come to the following equation for $\delta\varphi$:

$$\begin{aligned} & \delta\varphi'' - 2\delta\varphi' \left(\tan 2\eta + \frac{1}{\cos 2\eta \sin 2\eta} \right) \\ & - \sqrt{\frac{3m_P^2}{4\pi}} m^2 a_0^2 \left(\frac{\cos 2\eta}{16 \sin 2\eta} \ln^2 \frac{1 + \sin 2\eta}{1 - \sin 2\eta} - \frac{\cos 2\eta}{4} \ln \frac{1 + \sin 2\eta}{1 - \sin 2\eta} \right) = 0 \end{aligned} \quad (3.17)$$

This equation can be integrated and its solution looks as follows:

$$\begin{aligned} \delta\varphi' = & \sqrt{\frac{3m_P^2}{4\pi} \frac{m^2 a_0^2}{16} \frac{\sin 2\eta}{\cos^2 2\eta}} \times \left\{ 2 \sin 2\eta \right. \\ & - \frac{1 + \sin^2 2\eta}{2 \sin 2\eta} \ln^2 \frac{1 + \sin 2\eta}{1 - \sin 2\eta} - \cos^2 2\eta \ln \frac{1 + \sin 2\eta}{1 - \sin 2\eta} + \ln^2(1 - \sin 2\eta) - \ln^2(1 + \sin 2\eta) \\ & \left. + 2 \ln 2 \ln \frac{1 + \sin 2\eta}{1 - \sin 2\eta} + 2 Li_2 \left(\frac{1 - \sin 2\eta}{2} \right) - 2 Li_2 \left(\frac{1 + \sin 2\eta}{2} \right) + C \right\}. \end{aligned} \quad (3.18)$$

Here, in Eq. (3.18) $Li_2(x)$ is dilogarithm function, which can be defined as a series

$$Li_2(x) \equiv \sum_{n=1}^{\infty} \frac{x^n}{n^2}.$$

The constant of integration C in Eq. (3.18) should be chosen equal to zero to provide the satisfaction of the condition

$$\delta h(0) = 0,$$

which means that the first-order correction to $h^{(0)}$ that can be obtained by substitution of Eq. (3.18) into Eq. (3.16) should not destroy the initial conditions for our evolution, i.e. that the beginning of our consideration coincides with the point of maximal expansion.

The behavior of δh and $\delta\varphi'$ are presented in Fig. 6a and 6b respectively. We see that $\delta\varphi'$ begins since zero value monotonically decreasing and tending to $-\infty$ at $\eta \rightarrow \pi/4$, while δh beginning since zero value monotonically increases and tends to $+\infty$ at $\eta \rightarrow \pi/4$. Both first corrections have opposite signs in respect with the corresponding functions in zero approximation. So one can say that inclusion of the first corrections $\delta\varphi'$ and δh can describe the transition from the set of trajectories without bounces and φ -turns to those, having more complicated structure. It is interesting also to depict the plots for the relative values $\frac{\delta\varphi'}{\varphi^{(0)}}$ and $\frac{\delta h}{h^{(0)}}$ which are presented in Fig. 6c. The absolute value of $\frac{\delta h}{h^{(0)}}$ is everywhere more than that of

$\frac{\delta\varphi'}{\varphi^{(0)'}}$. It means that we have bounce earlier than φ -turn and in such a way our perturbative scheme describes the transition from the region **0** to the region **1** described in the preceding section. (It looks quite natural that due to the first approximation of our perturbative scheme we can describe only the small part of the general set of trajectories, besides the regions disposed to the right from the region **1** correspond to the comparatively large values of our parameter $m^2 a_0^2$ and hardly can be described by perturbative methods).

However, here we should recognize that our perturbative scheme fails in the vicinity of singularity. Indeed, it is enough to look at the Fig. 6c to understand that $\frac{\delta h}{h^{(0)}}$ reaches the value -1 at *any* value of the parameter ma_0 that means that we shall have bounce on every trajectory independently of the initial conditions. However, we know that at small values of the radius of maximal expansion a_0 we have the trajectories lying in the region **0**, i.e. the trajectories without bounces and φ -turns. Thus, we see that we can not, unfortunately, to estimate the parameters characterising the change of the regimes of the behavior of our trajectories using our perturbative scheme, because this scheme does not work in the vicinity of singularity. However, one can try to extract some useful information combining the perturbative results, numerical methods and the equations describing the location of possible points of maximal expansion and minimal contraction presented in the preceding section (see also Ref. 9).

First of all let us consider the symmetric trajectories, i.e trajectories whose points of maximal expansion lies at $\varphi = 0$. Numerical calculations show that the boundary between the regions **0** and **1** lies at

$$ma_0 \text{ numerical} = 2.3. \tag{3.19}$$

Now one can try to find this value using zero approximation of our perturbative scheme or in other words, using the exact solutions of the equations of massless model given by formulas (3.5)–(3.8). Naturally, these equations describe the trajectories without bounces, however, we can put forward the suggestion that zero-approximation becomes invalid and the trajectories can have bounce when these trajectories come into the region where points of minimal contraction are localized, i.e. where according to Eq. (2.10)

$$\varphi a \geq \sqrt{\frac{1}{2\pi}} \frac{m_P}{m}. \quad (3.20)$$

Substituting into Eq. (3.20) expressions for $\varphi(\eta)$ and $a(\eta)$ from Eqs. (3.8) and (3.5) we have

$$ma_0 \geq \frac{4\sqrt{\frac{2}{3}}}{\sqrt{\cos 2\eta} \ln \frac{1+\sin 2\eta}{1-\sin 2\eta}}. \quad (3.21)$$

The value of ma_0 separating the regions **0** and **1** can be found from the comparison of left-hand-side of non-equality (3.21) with the maximal value of its right-hand-side. This value is as follows:

$$ma_0 \text{ zero approximation} = 1.6. \quad (3.22)$$

Now one can try to estimate the same value of the parameter ma_0 separating the regions **0** and **1** using the first perturbative corrections to a and φ . The logic of this estimation will be in a way an opposite to that used in the manipulation with zero-order (massless) solutions. Indeed, working in zero-order approximation of the perturbation theory we have only the trajectories without bounces. However, we know in that in some region of our configuration space we can have bounces in the *full* theory. Thus, fixing the moment when our “zero-order” trajectories come into this region we can estimate the value of the parameter ma_0 giving the boundary

between the regions **0** and **1**. In first approximation *all* the trajectories have a bounce at the moment when $\delta h = -h^{(0)}$, but we can again estimate the value φa at the moment of bounce and to check if it satisfies the non-equality (3.20). At some small values of ma_0 this non-equality is broken and in such a way we can estimate the boundary value of ma_0 . Of course, these calculations are much more complicated than those for zero-order approximation and need some help of numerical methods. It is interesting that the value of ma_0 parameterizing the boundary between regions **0** and **1** is

$$ma_0 \text{ first approximation} = 1.8 \tag{3.23}$$

and it is closer to the value obtained in the framework of full theory (see Eq. (3.19)) than the value obtained in the framework of zero-order approximation (see Eq. (3.22)). Thus one can say that up to some extent our perturbation theory complemented by some qualitative considerations describes the transitions between different types of trajectories presented in the full theory. We would like to hope that the developed here perturbative scheme can be useful in other problems where we have opportunity to consider the exactly solvable model which is in some kinship with the model under consideration.

ACKNOWLEDGMENTS

We are grateful to D.N. Page and V. Sahni for useful discussions. This work was supported by Russian Foundation for Fundamental Researches via grants No 96-02-16220 and No 96-02-17591 and by INTAS via project 93-3364-Ext. I.M.K. is grateful to School of Physics and Astronomy Tel Aviv University for constant support.

1. A.D. Linde, *Particle Physics and Inflationary Cosmology* (Harwood Academic, 1990) and references therein.
2. J.B. Hartle and S.W. Hawking, *Phys. Rev.* **D28**, 2960 (1983); S.W. Hawking, *Nucl. Phys.* **B239**, 257 (1984).
3. A. Vilenkin, *Phys. Lett.* **117B**, 25 (1982); *Phys. Rev.* **D27**, 2848 (1983); *Phys. Rev.* **D30** 509 (1984); *Phys. Rev.* **D37**, 888 (1988); A.D. Linde, *Zh. Eksp. Teor. Fiz.* **87**, 369 (1984) [*Sov. Phys. JETP* **60**, 211 (1984)]; Ya.B. Zeldovich and A.A. Starobinsky, *Pis'ma Astron. Zh.* **10**, 323 (1984) [*Sov. Astron. Lett.* **10**, 135 (1984)]; V.A. Rubakov, *Phys. Lett.* **148B**, 280 (1984).
4. A.O. Barvinsky, *Phys. Rep.* **230**, 237 (1993); A.O. Barvinsky and A.Yu. Kamenshchik, *Phys. Rev.* **D50**, 5093 (1994).
5. B.L.Spokoiny, *Phys. Lett.* **129B**, 39 (1984); D.S. Salopek, J.R. Bond and J.M. Bardeen, *Phys. Rev.* **D40**, 1753 (1989); R. Fakir and W.G. Unruh, *Phys. Rev.* **D41**, 1783 (1990); R. Fakir, S. Habib and W.G. Unruh, *Aph. J.* **394**, 396 (1992); R. Fakir and S. Habib, *Mod. Phys. Lett.* **A8**, 2827 (1993).
6. I.M. Khalatnikov and A. Mezhlumian, *Phys. Lett.* **A169**, 308 (1992); I.M. Khalatnikov and P. Schiller, *Phys. Lett.* **B302**, 176 (1993).
7. L. Amendola, I.M. Khalatnikov, M. Litterio and F. Occhionero, *Phys. Rev.* **D49**, 1881 (1994).
8. A.Yu. Kamenshchik, I.M. Khalatnikov and A.V. Toporensky, *Phys. Lett.* **B357**, 36 (1995).

9. A.Yu. Kamenshchik, I.M. Khalatnikov and A.V. Toporensky, *Int. J. Mod. Phys.* **D** (in press) // gr-qc/9801039.
10. V.A. Belinsky, L.P. Grishchuk, Ya.B. Zel'dovich and I.M. Khalatnikov, *J. Exp. Theor. Phys.* **89**, 346 (1985).
11. V.A. Belinsky and I.M. Khalatnikov, *J. Exp. Theor. Phys.* **93**, 784 (1987);
V.A. Belinsky, H. Ishihara, I.M. Khalatnikov and H. Sato, *Progr. Theor. Phys.* **79**, 676 (1988).
12. G.A. Burnett, *Phys. Rev.* **D51**, 1621 (1995).
13. S.W. Hawking, in *Relativity, Groups and Topology II*, ed. B.S. DeWitt and R. Stora, (North Holland, Amsterdam, 1984).
14. D.N. Page, *Class. Quantum Grav.* **1**, 417 (1984).
15. L. Parker and S.A. Fulling, *Phys. Rev.* **D7**, 2357 (1973); A.A. Starobinsky, *Pisma A.J.* **4** 155 (1978).
16. V.A. Belinsky and I.M. Khalatnikov, *J. Exp. Theor. Phys.* **63**, 1121 (1972).
17. R. de Ritis, G. Marmo, G. Platania, C. Rubano, P. Scudellaro and C. Stornaiolo, *Phys. Rev.* **D42**, 1091 (1990); *Phys. Lett.* **149A**, 79 (1990); S. Capozziello, R. de Ritis and P. Scudellaro, *Int. J. Mod. Phys.* **D3**, 609 (1994); J.D. Barrow, *Phys. Rev.* **D49**, 3055 (1994); F.E. Schunk and E.W. Mielke, *Phys. Rev.* **D50**, 4794 (1994); S. Capozziello, M. Demianski, R. de Ritis and C. Rubano, *Phys. Rev.* **D52**, 3288 (1995).
18. B. Mandelbrot, *The fractal geometry of nature*, (San Francisco, Freeman, 1982).

19. G.W. Lyons, *Phys. Rev.* **D46**, 1546 (1992); R. Bousso and S.W. Hawking, *Phys. Rev.* **D52**, 5659 (1995); A.O. Barvinsky, A.Yu. Kamenshchik and I.V. Mishakov, *Nucl. Phys.* **B491**, 387 (1997).
20. M. Abramowitz and I.A. Stegun, *Handbook of mathematical functions*, (New York, Dover, 1972).

Captions to Figures

Fig. 1. On the half-plane $a \geq 0, \varphi$ the solid hyperbolic curves are those separating Lorentzian region from Euclidean one. Dashed hyperbolic curves separate the possible points of maximal expansion $\dot{a} = 0, \ddot{a} < 0$ (these points can exist between two branches of dashed curves) and the possible points of minimal contraction $\dot{a} = 0, \ddot{a} > 0$ (these points can exist between the dashed and solid hyperbolic curves).

Fig. 2. The structure of the region of the localization of possible points of maximal expansion is presented. We consider here the points of maximal expansion corresponding to the trajectories which at these points has the direction “up”, i.e. $\dot{\varphi} > 0$.

The region **0** corresponds to the trajectories which after going through the point of maximal expansion placed in this region go to the singularity $a = 0, \varphi = +\infty$.

The region **1** corresponds to the trajectories which after the going through the points of maximal expansion have a point of minimal contraction or “bounce”.

The region **1'** corresponds to the trajectories which after the going through the point of maximal expansion have a φ -turn, i.e. the point where $\dot{\varphi} = 0$ after that they fall to singularity $a = 0, \varphi = -\infty$.

The region **2** corresponds to the trajectories which after the going through the point of maximal expansion and subsequent φ - turn have bounce.

The region **2'** corresponds to the trajectories which after going through the point of maximal expansion and two subsequent φ - turns fall to singularity and so on.

We did not depicted the regions $\bar{1}, \bar{2}, \dots$ described in the main text. These

regions are included into regions $\mathbf{1}'$, $\mathbf{2}'$, \dots correspondingly.

Fig. 3. The parts of the trajectories corresponding to the regions presented on the preceding Figure are depicted. We trace out for the sake of simplicity of the classification only the pieces of these trajectories beginning since the point of maximal expansion ignoring their “prehistories”. On the **Fig. 3a – 3h** we consider the trajectories whose points of maximal expansion are placed at the line $\varphi = 0$, though it is not essential from the general point of view.

In **Fig. 3a** is presented the trajectory corresponding to the region $\mathbf{0}$ falling after the point of maximal expansion to the singularity.

In **Fig. 3b** the trajectory corresponding to the region $\mathbf{1}$ is presented. This trajectory has a bounce after the going through the point of maximal expansion.

In **Fig. 3c** is presented the periodic trajectory having two symmetric points of “full stops” $\dot{a} = 0, \dot{\varphi} = 0$ at the boundary between Lorentzian and Euclidean regions and the point of maximal expansion placed just at the boundary between the regions $\mathbf{1}$ and $\mathbf{1}'$ (or, to be precise on the boundary between the regions $\mathbf{1}$ and $\bar{\mathbf{1}}$).

In **Fig. 3d** the trajectory corresponding to the region $\bar{\mathbf{1}}$ is presented. This trajectory after the point of maximal expansion has φ - turn, almost immediately after it – bounce, then the second point of maximal expansion and then it goes to singularity.

In **Fig. 3e** we have the trajectory corresponding to the region $\mathbf{1}'$ which after φ - turn falls to infinity.

In **Fig. 3f** we see the trajectory corresponding to the region $\mathbf{2}$ which after the φ - turn has a bounce already in the lower half-plane.

In **Fig. 3g** we see the periodic trajectory whose point of maximal expansion

lies on the axes $\varphi = 0$ just at the boundary between the regions **2** and $\bar{2}$.

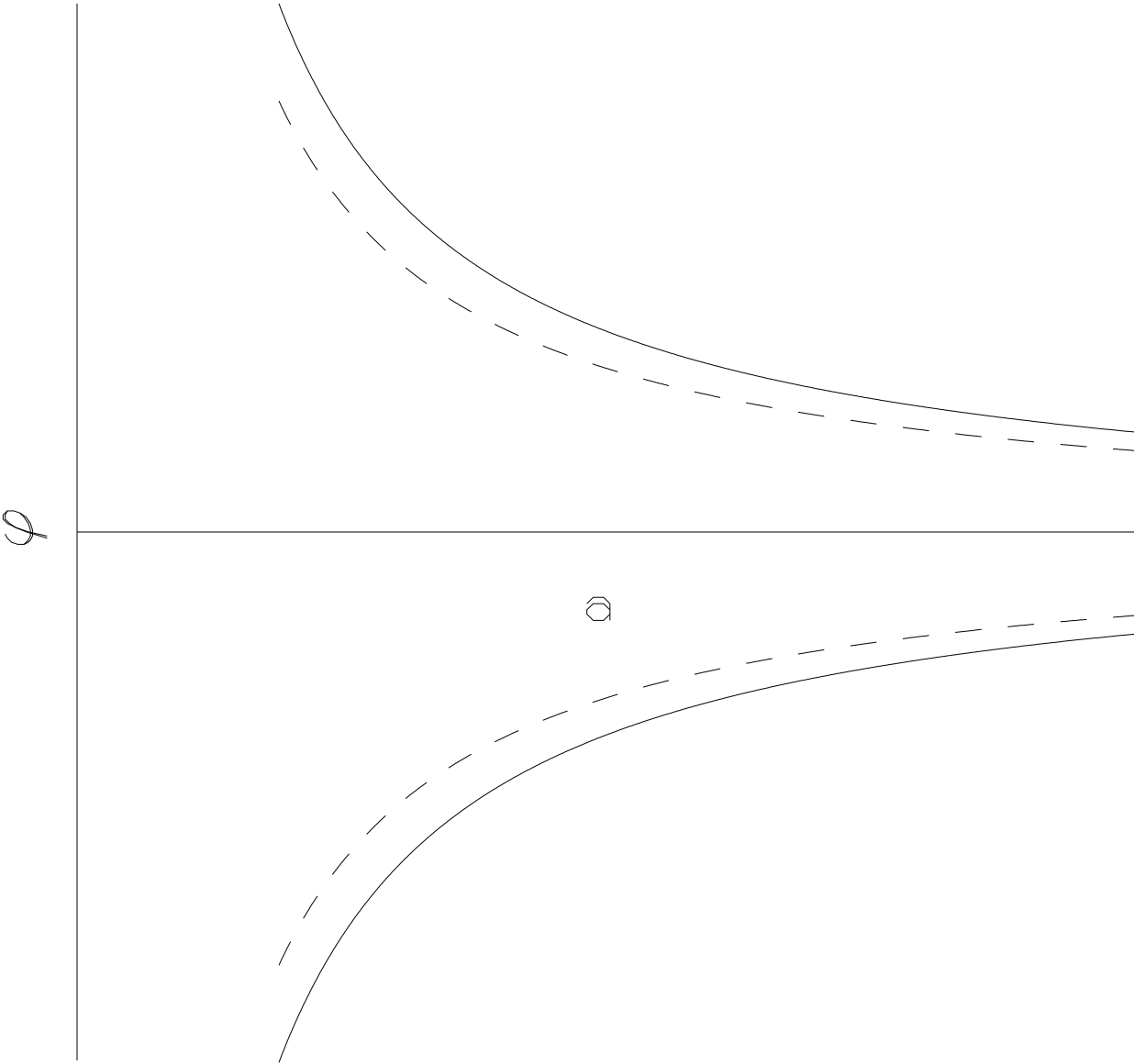
In **Fig. 3h** is shown the trajectory corresponding to the region **2'** which after two φ - turns fall to upper singularity.

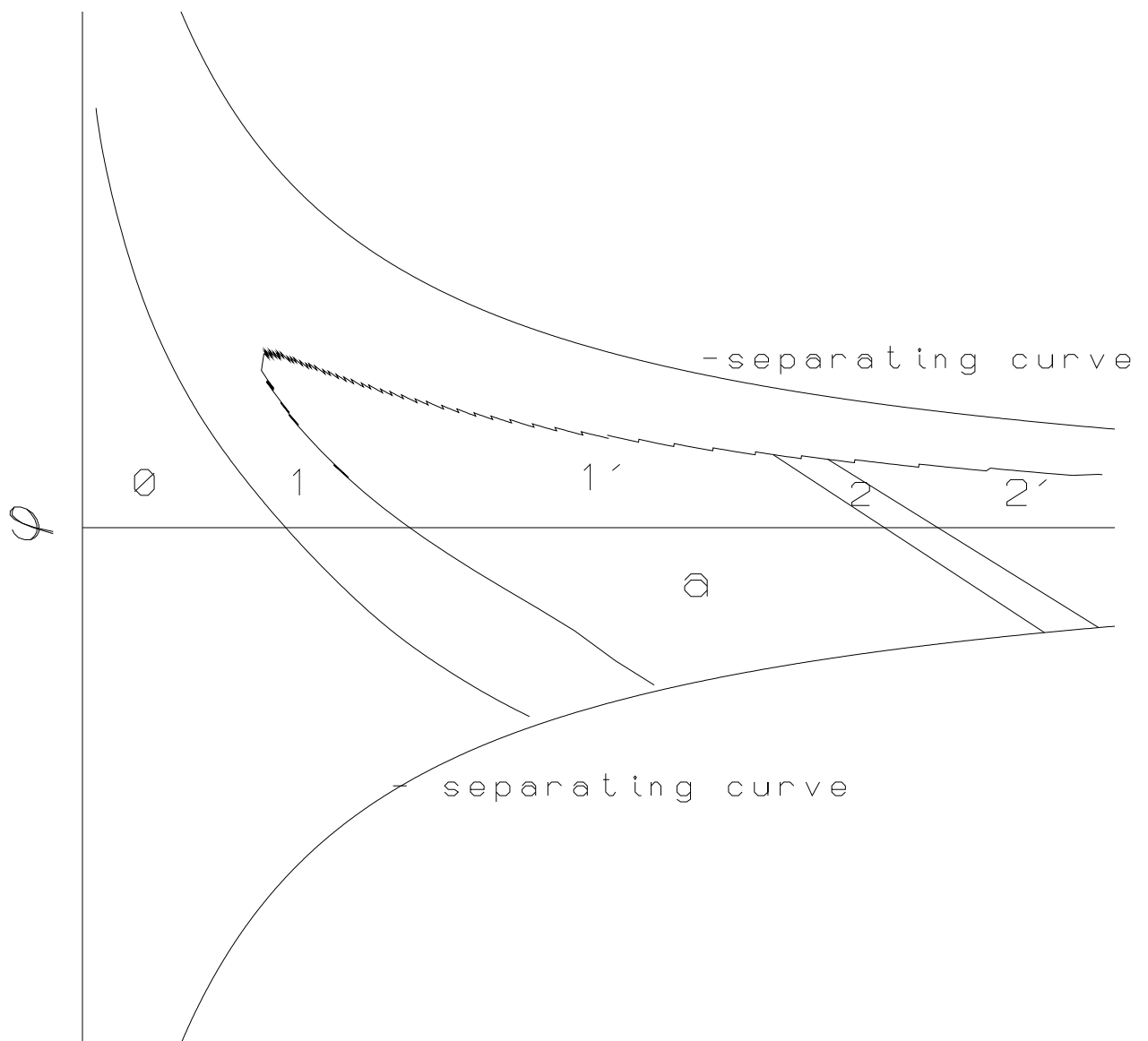
In **Fig. 3i** is shown the trajectory whose point of maximal expansion is placed in the upper branch of the region **1**. This trajectory immediately after the bounce has φ - turn, then goes through the second point of maximal expansion falls into singularity in the lower half-plane.

Fig. 4. The structure of the subregions of the region **1** is presented. Thin regions denoted by letters “b,c,d,e” correspond to the trajectories which have at least two bounces. The subregion “a” and other subregions placed between thin regions correspond to the trajectories falling to singularity after one bounce.

Fig. 5. The trajectories corresponding to different subregions of the region **1** are presented. The trajectories depicted on the **Fig. 5a – 5e** correspond respectively to the subregions “a–e” presented in **Fig. 4**. The trajectory depicted on **Fig. 5a** has only one bounce while the trajectories have at least two bounces. The trajectories shown in **Fig. 5c** and **Fig. 5e** have a point of full stop (or at least are very close to it).

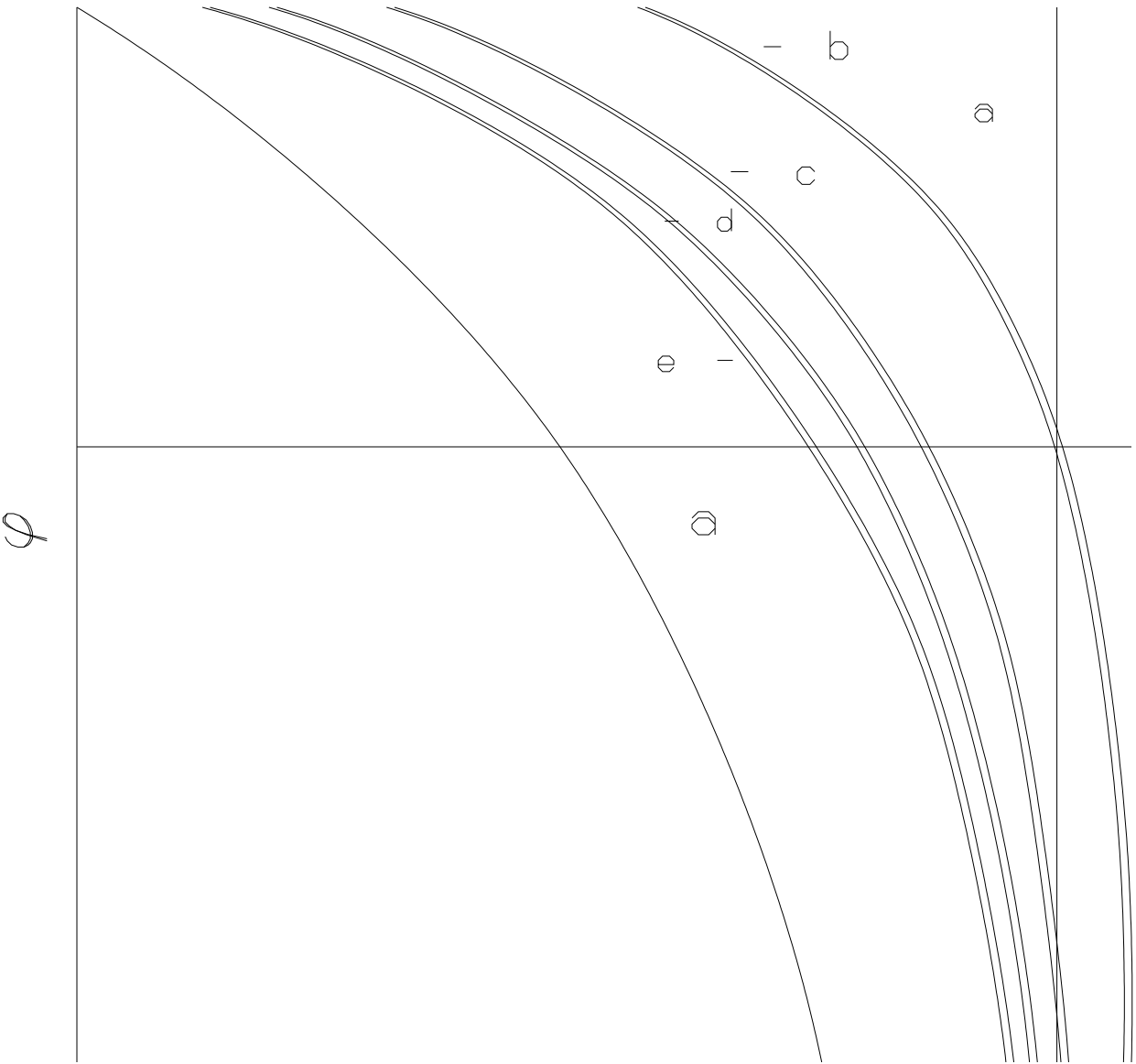
Fig. 6. In **Fig. 6a** is presented the dependence of the δh on the conformal time η while in **Fig. 6b** the dependence of $\delta\varphi'$ on η is presented. In **Fig. 6c** solid line shows the behavior of $\delta h/h$ and dashed line shows the behavior of $\delta\varphi'/\varphi'$.





This figure "simpl3.gif" is available in "gif" format from:

<http://arxiv.org/ps/gr-qc/9801064v1>



This figure "simpl5.gif" is available in "gif" format from:

<http://arxiv.org/ps/gr-qc/9801064v1>

